Solid-phase approaches for labelling targeting peptides with far-red emitting coumarin fluorophores

Anna Rovira,[†,§] Albert Gandioso,[†,§] Marina Goñalons,[†] Alex Galindo,[†] Anna Massaguer,[‡] Manel Bosch,[⊥] and Vicente Marchán*[,†]

[†]Departament de Química Inorgànica i Orgànica, Secció de Química Orgànica, IBUB, Universitat de Barcelona, Martí i Franquès 1-11, E-08028 Barcelona (Spain).

[‡]Departament de Biologia, Universitat de Girona, E-17071 Girona (Spain).

[⊥]Unitat de Microscòpia Òptica Avançada, Centres Científics i Tecnològics, Universitat de Barcelona, E-08028 Barcelona (Spain)

[§]These authors contributed equally to this work.

TOC ABSTRACT GRAPHIC

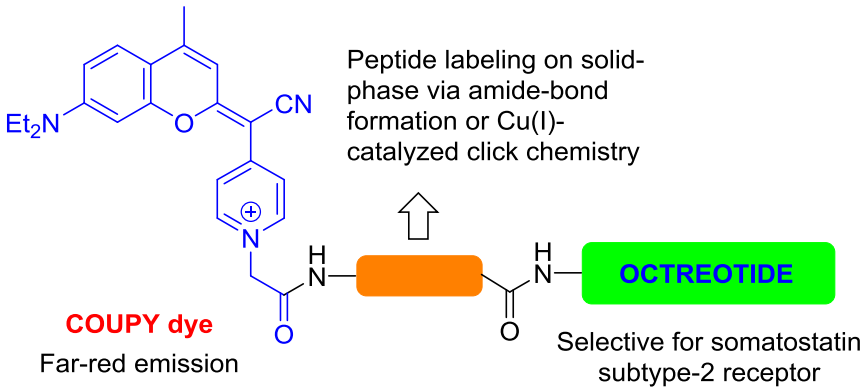

ABSTRACT

Fluorophores based on organic molecules hold great potential for ligand-targeted imaging applications, particularly those operating in the optical window in biological tissues. In this work we have developed three straightforward solid-phase approaches based on amide-bond formation or Cu(I)-catalyzed azide–alkyne click (CuAAC) reaction for labelling octreotide peptide with far-red emitting coumarin-based COUPY dyes. First, the conjugatable versions of COUPY fluorophores incorporating the required functional groups (e.g., carboxylic acid, azide or alkyne) were synthesized and characterized. All of them were found fully compatible with Fmoc/*t*Bu solid-phase peptide synthesis, which allowed the labeling of octreotide either through amide-bond formation or by CuAAC reaction. A near quantitative conversion was obtained after only 1 h of reaction at RT when using $CuSO_4$ and sodium ascorbate independently of the click chemistry approach used (azido-COUPY/alkynyl-peptide resin or alkynyl-COUPY/azido-peptide resin). COUPY-octreotide conjugates were found stable in cell culture medium as well as non-cytotoxic in HeLa cells, and their spectroscopic and photophysical properties were found similar to those of their parent coumarin dyes. Finally, the potential bioimaging applications of COUPY-octreotide conjugates were demonstrated by confocal microscopy through the visualization of living HeLa cells overexpressing somatostatin subtype-2 receptor.

INTRODUCTION

Last few decades have witnessed an impressive growth in the development of novel therapeutic and diagnostic technologies against cancer. In this context, receptors over-expressed on cancer cells have been exploited to selectively deliver a large variety of cytotoxic drugs with the aim of minimizing toxic side-effects associated with chemotherapy. Ligand-targeted imaging agents also offer great potential in the early detection of cancerous cells, as well as in fluorescence-guided surgery (FGS), which allows resection of solid tumours after illumination of malignancies directly in the operating room.[1] Recent advances in fluorophore chemistry and knowledge of targetable receptors have led to the clinical testing of several targeted fluorophores for intraoperative cancer detection and FGS.[1b,2]

Owing to the potential of fluorophores based on organic molecules in ligand-targeted imaging applications, it is urgent to develop novel low molecular-weight fluorescent probes operating in the far-red and near-infrared (NIR) region, since only the use of non-toxic and high tissue-penetrating radiation will guarantee clinical translation in the next years.[3] Ideally, such fluorophores should be amenable to smart structural modifications to tune, on demand, photophysical and physicochemical properties, as well as to facilitate conjugation to a broad variety of targeting ligands (e.g., peptides, proteins, folic acid, monoclonal antibodies (mAb), etc.) by using efficient and chemoselective conjugation chemistries. Although many times forgotten, the biological properties of a targeting ligand should not be impaired by the fluorescent tag. This issue is particularly problematic in the case of short peptide sequences since uptake and subcellular localization may be strongly influenced by the fluorophore.[4] In the same way, some structural modifications of cyanine-based dyes have been reported to alter the mechanism of mAb when conjugated together, and non-specific hydrophobic interactions between Epidermal Growth Factor (EGF) receptor and the dye moiety in BODIPY-peptide conjugates were found to reduce peptide-receptor binding specificity.[5] Hence, the choice of the fluorophore cannot be underestimated since constitutes a critical parameter in ligand-targeted imaging applications.

Recently, we have developed a novel family of coumarin-based fluorophores, nicknamed COUPYs, with promising photophysical properties and great potential for imaging applications.[6] As shown in Figure 1, replacement of the carbonyl function in coumarin **1** with the cyano(4-pyridine)methylene moiety (e.g., compound **2**) allowed us to increase the push−pull character of the conventional coumarin chromophore, which was easily transformed into pH-independent far-red/NIR-emitting fluorophores through *N*-alkylation of the pyridine heterocycle (e.g., compound **3**). Although the photostability of COUPY dyes can

be tuned through the incorporation of CF_3 groups at the coumarin skeleton[6] or by replacement of *N*,*N*-dialkylamino groups at position 7 with the four membered ring azetidine,[6b] the electron-withdrawing cyano group might also have a role in their photostability as previously demonstrated in some cyanine derivatives and in other dyes.[7] Considering the small size and the easy synthetic accessibility to COUPY dyes, these compounds are potential candidates for labelling targeting ligands such as receptor-binding peptides. In such a context, we envisaged that conjugatable versions of COUPY dyes (e.g., compounds **4** to **6** in Figure 1) could be obtained from scaffold **2** through *N*-alkylation with adequate reagents, thereby providing suitable functional groups (e.g., carboxylic acid, azide or alkyne) for conjugation via amide-bond formation or copper(I)-catalyzed azide–alkyne cycloaddition reaction (CuAAC), respectively.[8]

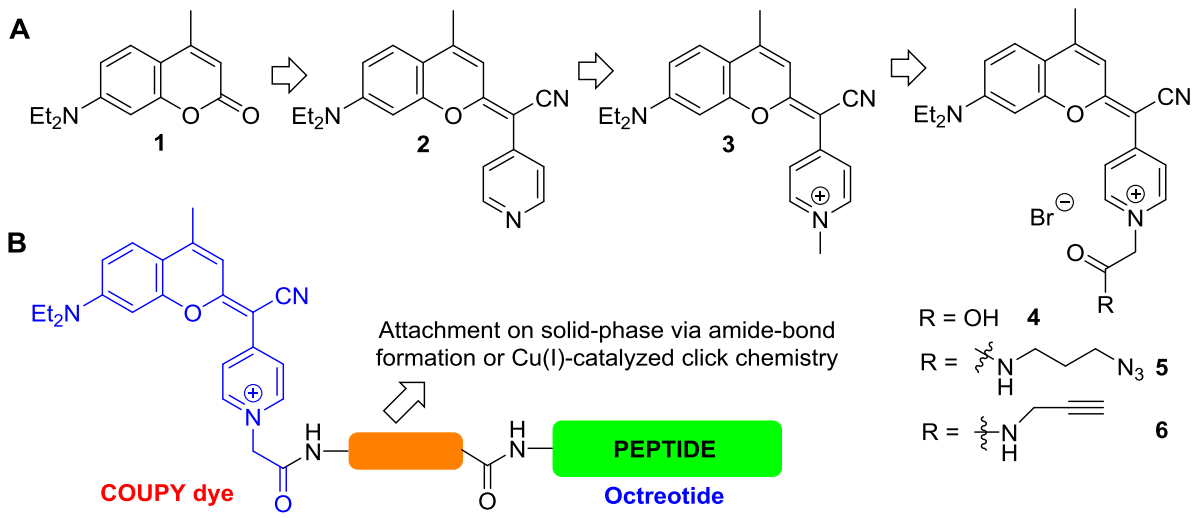

Figure 1. Rational design of conjugatable versions of COUPY dyes (A) and schematic representation of COUPY-octreotide conjugates (B).

Herein, we report for the first time three straightforward solid-phase approaches for the conjugation of coumarin-based COUPY fluorophores to octreotide, a FDA-approved peptide that displays high affinity and selectivity for somatostatin receptors, mainly subtype-2 receptor (SSTR2) which is overexpressed on the membrane of various types of malignant cells.[9] This cyclic octapeptide is a promising candidate for developing novel targeted imaging agents since some derivatives, such as [^{111}In-DTPA]- and [^{90}Y-DOTA-Tyr3]-octreotide conjugates, are routinely used in the clinics for molecular imaging and therapy of neuroendocrine tumors, respectively, and several other SSTR2-targeted radiotherapeutics are currently under clinical evaluation.[1a] Octreotide has also been conjugated successfully to

several anticancer drugs (both organic compounds and metallodrugs),[10] including Ir(III) complexes useful for theranostic applications.[11]

RESULTS AND DISCUSSION

Synthesis and characterization of conjugatable COUPY dyes.

COUPY fluorophores **4-6** were easily synthesized through *N*-alkylation of **2** (Scheme 1), which was previously obtained by condensation of thiocoumarin **7**[6,12] with 4-pyridylacetonitrile. On the one hand, reaction of **2** with methyl bromoacetate afforded intermediate **8** in excellent yield after silica column chromatography (97%). This compound was transformed into coumarin **4** bearing the carboxylic acid function by acidic hydrolysis (Figure S1). On the other hand, azido- (**5**) and alkynyl- (**6**) containing fluorophores were synthesized by reaction of **2** with *N*-alkyl bromoacetamide derivatives containing the appropriate functional groups for CuAAC (compounds **9** and **10**, respectively). Compounds **5** and **6** were obtained as dark blue solids after purification (96% and 80% yields, respectively). Full characterization was carried out by HR ESI-MS and 1D (^{1}H and ^{13}C) and 2D NMR, and the purity was assessed by reversed-phase HPLC (Figure S1). Similarly to the parent COUPY dye **3**, NOESY experiments revealed that the *E* rotamer was the major species in solution (Figures S2-S4).[6]

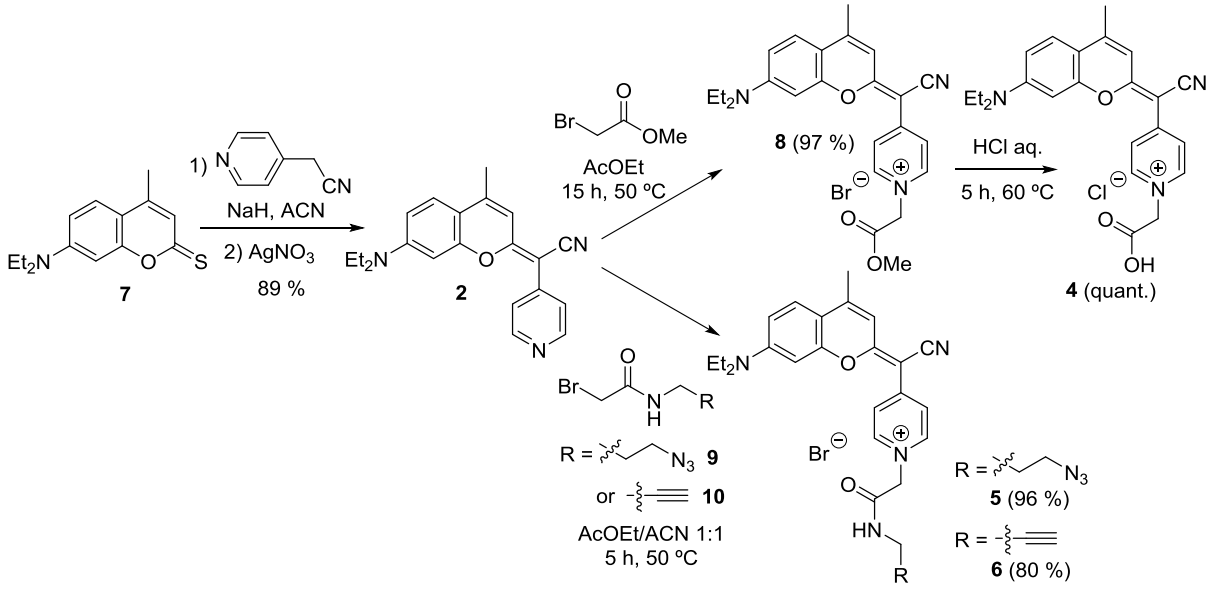

Scheme 1. Synthesis of conjugatable COUPY dyes **4-6.**

Synthesis and characterization of COUPY-octreotide conjugates.

Having at hand the conjugatable COUPY derivatives (**4-6**), we focused on labelling octreotide following a stepwise solid-phase strategy since it allows the regioselective attachment of the fluorescent dye at the *N*-terminal end of the peptide sequence, either through amide-bond formation or by Cu(I)-catalyzed click chemistry. First, the linear octapeptide sequence

incorporating a short polyethylenglycol spacer (**11**) was assembled manually on a Rink amide resin-*p*-MBHA using standard Fmoc-*t*Bu methodology (Scheme 2). After coupling of coumarin **4** with HATU in the presence of DIPEA, side-chain deprotection and cleavage from the resin (TFA/TIS/H_2O/EDT 94:2.5:2.5:1, 2.5 h RT) and cyclization via disulfide bond formation in an aqueous buffer (pH 7-8) were carried out. Analysis by HPLC-ESI MS showed a main peak (Figure S5) that was isolated and characterized as the expected COUPY-octreotide conjugate (**12**). Finally, after purification by semipreparative HPLC and lyophilization, the formate salt of **12** (overall yield 12%) was obtained as a pink solid and fully characterized by HR ESI-MS and NMR. As shown in Figure S6, the obtained *m/z* values are consistent with the calculated values of the charged species $[M]^+$, $[M+H]^{2+}$ and $[M+2H]^{3+}$. In addition, the aromatic region of the ^1H NMR spectra in 8:2 H_2O/D_2O-DMSO-d_6 mixtures showed diagnostic peaks from the fluorophore and the peptide (amide NH protons and aromatic protons of *D/L*-Phe and *D*-Trp residues), confirming the covalent attachment of both moieties (Figure 2). Importantly, conjugate **12** was found stable in cell culture medium (DMEM supplemented with 10 % FBS) after incubation for 24 h (Figure S7), as well as non-cytotoxic in HeLa cells (Figure S8). Both pre-requisites are necessary for exploring the bioimaging applications of COUPY-peptide conjugates.

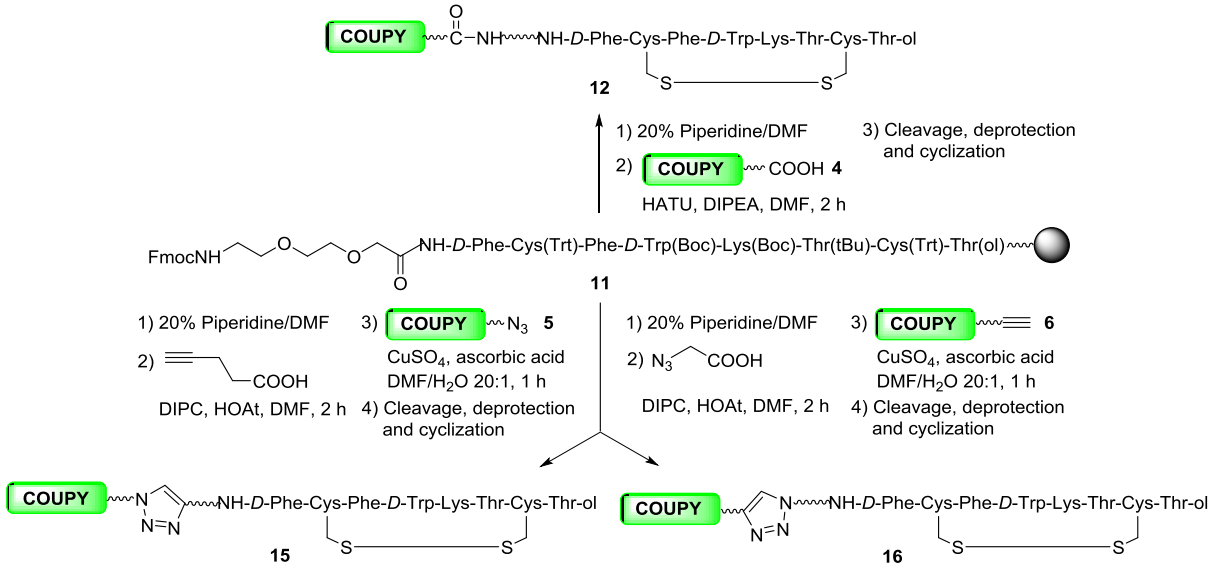

Scheme 2. Schematic representation of the three solid-phase approaches used for labelling octreotide with COUPY dyes via amide-bond formation (top) or CuAAC reaction (bottom).

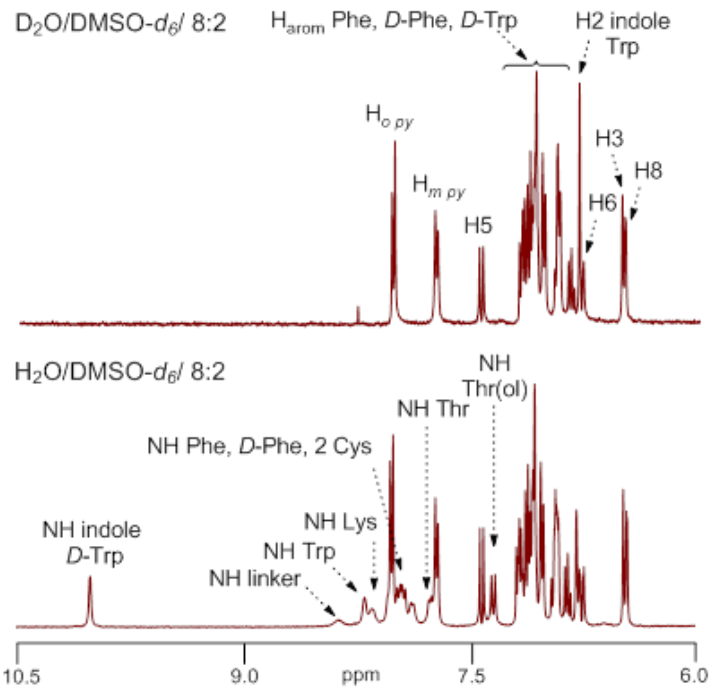

Figure 2. Aromatic region of the ^{1}H NMR spectra of conjugate **12** in D_2O-DMSO-d_6 8:2 (top) and in H_2O-DMSO-d_6 8:2 (bottom).

Once demonstrated the compatibility of COUPY dyes with solid-phase peptide synthesis (SPPS), we investigated the potential applications of coumarin derivatives bearing azide (**5**) and alkynyl (**6**) functional groups for labelling octreotide via CuAAC reaction on solid-phase, since click chemistry is routinely employed for modifying peptides, oligonucleotides, small molecules and polymers.[13] First, the required functional groups were incorporated at the *N*-terminal end of peptide-bound resin **11** by coupling 4-pentynoic acid or 2-azidoacetic acid, which provided alkynyl- (**13**) and azido- (**14**) peptide-bound resins, respectively, (Figures S9-S10). Click chemistry was investigated by reacting **13** and **14** resins with **5** and **6**, respectively, in the presence of $CuSO_4$ (3 mol equiv.) and sodium ascorbate (3 mol equiv.) in DMF/H_2O 20:1 for 18 h (Scheme 2). To our delight, after cleavage and deprotection, HPLC-MS analysis revealed the formation of the expected linear COUPY-octreotide conjugates. Since no significant side reactions derived of the presence of sodium ascorbate and Cu(I) were detected, we decided not to explore the use of Cu-stabilizing ligands. Although most click chemistry procedures reported in the literature describe the use of long reaction times (12-48 h) and even microwave irradiation for labelling peptides with organic fluorophores,[13a] we obtained near quantitative conversions after only 1 h of reaction at RT (see Figures S11 and S14 for the HPLC-MS analyses after 1 h, 4 h and overnight reaction times),

independently of the click chemistry approach used (azido-COUPY/alkynyl-peptide resin or alkynyl-COUPY/azido-peptide resin). Finally, after cyclization and purification, clicked COUPY-octreotide conjugates (**15** and **16**) were obtained as pink solids (Figures S13-S14 and S15-S16).

Photophysical characterization of COUPY-octreotide conjugates.

The photophysical properties (absorption and emission spectra, molar absorption coefficients (ε), and fluorescence quantum yields (ϕ_F)) of COUPY-octreotide conjugates were studied in water and in PBS buffer, and compared with those of their respective coumarin precursors (see Table 1 and Figure 3 and Figures S17-S20). All the compounds showed an intense absorption band in the yellow-red part of the visible spectrum, being the wavelength absorption maximum slightly red-shifted with respect the parent dye **3** (e.g., λ_{abs} = 543 nm for **3** *vs* λ_{em} = 555 nm for **5-6** and **8** in H_2O) because of the additional electron-withdrawing effect of ester and amide functions. Similarly, the emission maximum was red-shifted by *ca* 10 nm (e.g., λ_{em} = 605 nm for **3** *vs* λ_{em} = 615 nm for **5-6** and **8** in H_2O) and, consequently, the Stokes's shifts remained around 60-62 nm. An additional red-shift in absorption (*ca* 4-6 nm) and emission (*ca* 3-5 nm) maxima occurred after conjugation to octreotide. As shown in Table 1, the ϕ_F of the conjugatable coumarin derivatives (**8** and **5-6**) in aqueous media was reduced when compared with **3** (e.g., ϕ_F = 0.066 for **5** *vs* ϕ_F = 0.15 for **3** in H_2O). However, a clear improvement in the fluorescent quantum yield of these fluorophores was achieved when conjugated to the peptide (e.g., ϕ_F = 0.066 for **5** *vs* ϕ_F = 0.19 for conjugate **15** in H_2O), independently of the chemical conjugation approach used.

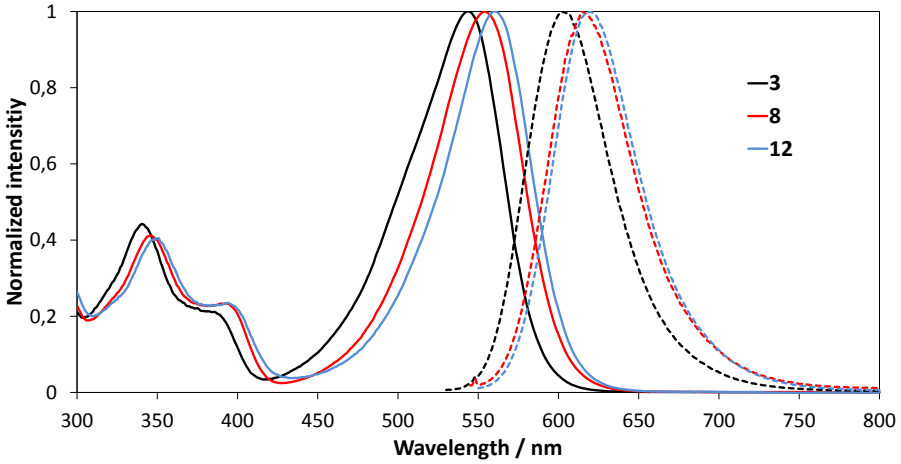

Figure 3. Comparison of the normalized absorption (solid lines) and fluorescence emission (dotted lines) spectra of coumarins **3** and **8** and of COUPY-octreotide conjugate **12**.

Table 1. Photophysical properties of COUPY dyes (**3**, **5**, **6** and **8**) and COUPY-octreotide conjugates (**12**, **15**-**16**) in PBS buffer and in H_2O. The data for coumarin derivative **3** has been included for comparison purposes.[6a]

	Solvent	**λ_{abs} (nm)**	**λ_{em} (nm)**	**Stokes' shift (nm)**	**ε ($mM^{-1}cm^{-1}$)**	**ϕ_F**
Coumarin **3**	PBS	543	603	60	34	0.14
	H_2O	543	605	62	31	0.15
Coumarin **8**	PBS	554	615	61	48	0.044
	H_2O	555	615	60	48	0.043
Coumarin **5**	PBS	554	616	62	47	0.063
	H_2O	555	615	60	50	0.066
Coumarin **6**	PBS	553	615	62	45	0.045
	H_2O	555	615	60	46	0.061
Conjugate **12**	PBS	561	620	59	24	0.14
	H_2O	561	618	57	27	0.17
Conjugate **15**	PBS	559	620	61	32	0.18
	H_2O	560	618	58	36	0.19
Conjugate **16**	PBS	559	618	59	26	0.14
	H_2O	560	618	58	30	0.19

Fluorescence imaging of COUPY-octreotide conjugates in living cells

Finally, we investigated the potential bioimaging applications of COUPY-octreotide conjugates. As a representative compound, we selected conjugate **12** and studied its cellular uptake by confocal microscopy in SSTR2-overexpressing HeLa cells after irradiation with a yellow light laser (λ_{ex} = 561 nm). Interestingly, fluorescent vesicles, mostly-like endosomes, were visible in the cytoplasm of all of the examined cells after 30 min of incubation with **12**, thereby confirming the internalization and accumulation of COUPY-octreotide conjugate in the cells (Figures 4 and S23). This pattern of staining contrasts with that of coumarin **3** (Figure S23), which accumulates preferentially in mitochondria and nucleoli,[6] and indicates that the internalization of COUPY-octreotide conjugate is driven exclusively by the peptide moiety and not by the coumarin tag. In order to get more insights into the cellular uptake of the conjugate, we incubated HeLa cells with **12** at 4 ^{o}C for 30 min. As shown in Figure 5, no staining was observed inside the cytoplasm, which confirms that **12** enters the cells only through an energy-dependent pathway. By contrast, the pattern of staining observed with **3** was not modified at low temperature (Figure 5), thereby suggesting internalization through simple passive diffusion.

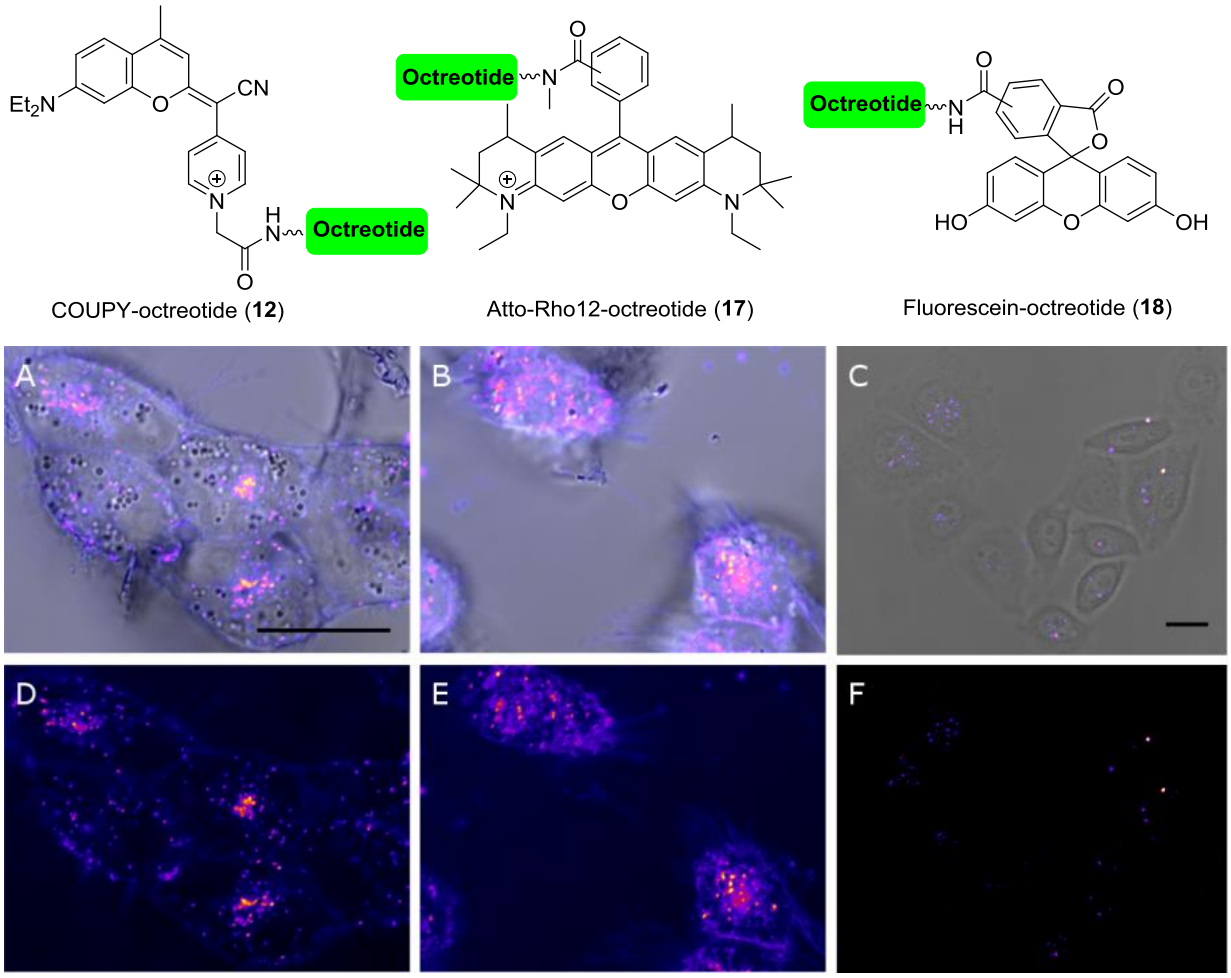

Figure 4. Comparison of the cellular uptake of COUPY- (**12**), Atto Rho12- (**17**) and Fluorescein- (**18**) octreotide conjugates. Top: structures of the conjugates. Bottom: single confocal planes of HeLa cells incubated with **12** (A and D) and **17** (B and E) at 10 μM and **18** (C and F) at 50 μM for 30 min at 37 ^{o}C. (A-C) Fluorescence images merged with bright field images. (D-F) Fluorescence images only. All fluorescence images are color coded using the Fire lookup table from Fiji. Scale bar: 20 μm. B,D,E same scale as A. F same scale as C.

Next, we decided to compare the visualization ability of COUPY dyes when conjugated to octreotide with that of two common commercially available fluorophores: 5(6)-carboxyfluorescein, which is one of the most popular fluorescent tags for labelling peptides and is typically excited at 488 nm, and Atto-Rho12, a rhodamine dye that can be excited with the same yellow light laser than our COUPY fluorophore. Atto-Rho12-octreotide (**17**) was synthesized by reaction of the corresponding succinimidyl ester derivative with octreotide and carboxyfluorescein-octreotide (**18**) was prepared by SPPS.[10b] As shown in Figure 4, the performance of the COUPY dye when conjugated to octreotide was comparable to that of the

rhodamine dye when exciting at 561 nm under similar conditions. By contrast, COUPY fluorophore allowed a much better visualization of HeLa cells than carboxyfluorescein, even at much lower concentrations and with a more convenient excitation wavelength (561 nm *vs* 488 nm). On the other hand, it is worth noting that conjugates involving carboxyfluorescein and Atto-Rho12 dyes (**17** and **18**) were obtained as regiomeric mixtures since both commercially available fluorophores are supplied as mixtures of isomers. However, COUPY-octreotide conjugate **12** was easily obtained as a single product, which represents a suitable alternative to many conventional fluorophores when labeled biomolecules with a well-defined structure are required for biological applications. Moreover, it is important to note that the photostability of COUPY-octreotide conjugate (**12**) in PBS buffer under green light irradiation (505 ± 15 nm; Figure 6) was found similar to that of the parent coumarin **3**,[6] which indicates that peptide derivatization through the pyridine heterocycle does not significantly modify the photostability of COUPY dyes.

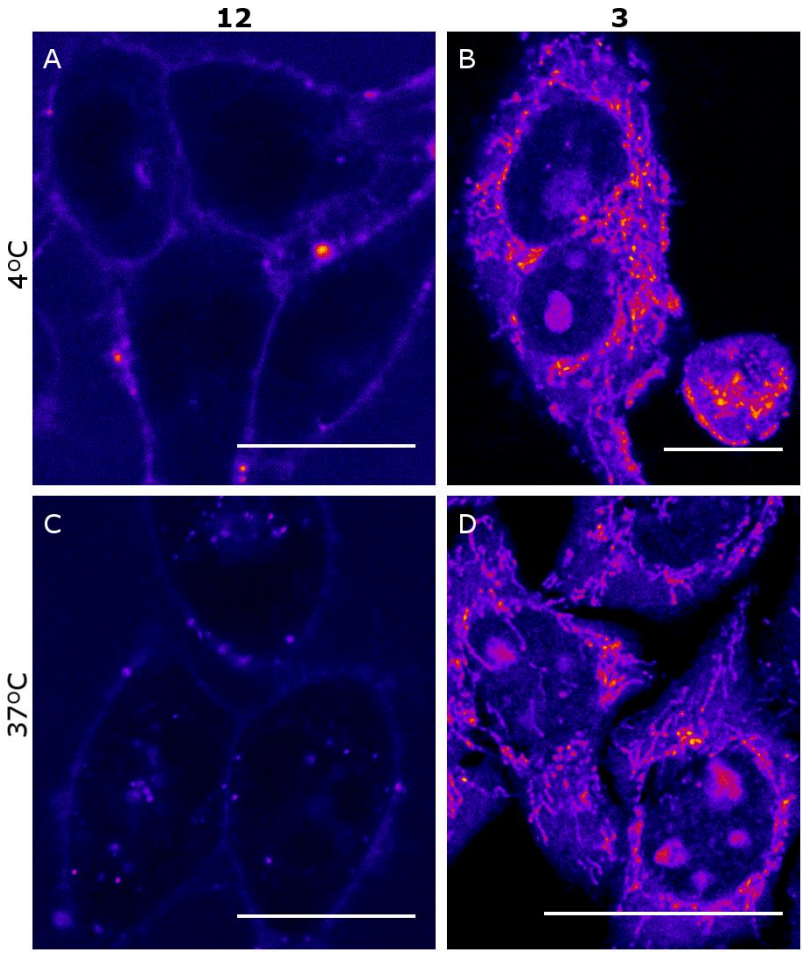

Figure 5. Comparison of the cellular uptake of COUPY-octreotide conjugate **12** and COUPY dye **3**. Single confocal planes of HeLa cells incubated with **12** (A and C) and **3** (B and D) at 10 μM or 0.5 μM, respectively, first at 4 ^{o}C for 30 min (A and B) and then incubated at 37 ^{o}C

for additional 30 min (C and D). The compounds were excited at 561 nm and emission detected from 570 to 670 nm. All images are color coded using the Fire lookup table from Fiji. Scale bar: 20 µm.

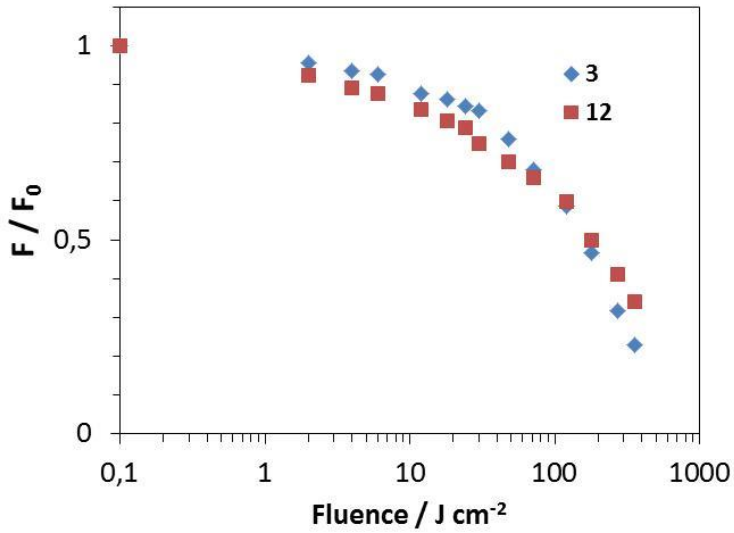

Figure 6. Fluorescence bleaching of COUPY-octreotide conjugate **12** and COUPY dye **3** in PBS buffer (5 µM) irradiated with green light (505 nm; 100 mW/cm^2).

CONCLUSIONS

In conclusion, we have synthesized three conjugatable versions of COUPY dyes (compounds **4** to **6**) incorporating suitable functional groups for conjugation via amide-bond formation (e.g., carboxylic acid) or copper(I)-catalyzed azide–alkyne cycloaddition (CuAAC) reaction (e.g., azide or alkyne). The compounds were easily obtained from a cheap, commercially available precursor, 7-*N*,*N*-diethylaminocoumarin, in only three or four linear steps, being the *N*-alkylation of the pyridine ring the key step. All the conjugatable coumarin derivatives were found fully compatible with Fmoc/*t*Bu solid-phase peptide synthesis, which allowed the straightforward labeling of octreotide peptide with a far-red emitting fluorophore. On the one hand, attachment of the coumarin **4** bearing a carboxylic acid function to the *N*-terminal end of the linear peptide-bound resin followed by acidic cleavage and deprotection and cyclization led to the expected COUPY-octreotide conjugate (**12**). This conjugate was found stable in cell culture medium as well as non-cytotoxic in HeLa cells. On the other hand, clicked COUPY-octreotide conjugates (**15** and **16**) were efficiently obtained by CuAAC reaction on solid-phase between azide- (**5**) and alkynyl- (**6**) containing COUPY dyes and peptide-bound resins containing the complementary functional groups.

The spectroscopic and photophysical properties of COUPY-octreotide conjugates were found similar to those of their parent coumarin dyes, being the wavelength absorption maximum located in the yellow-red part of the visible spectrum, while the emission ranged from the far red to the NIR region. Importantly, the fluorescent quantum yields of COUPY-octreotide conjugates in water were found higher than those of their coumarin precursors. Finally, the potential bioimaging applications of COUPY-octreotide conjugates were demonstrated by confocal microscopy in SSTR2-overexpressing living HeLa cells. Both the pattern of staining and the inhibition of the cellular uptake at low temperature indicate that the internalization of the conjugates is driven by the peptide moiety and not by the coumarin tag. Moreover, the fact that the visualization ability of COUPY dyes when conjugated to octreotide was similar to that of a commercially available rhodamine fluorophore, Atto-Rho12, and much better than that of the 5(6)-carboxyfluorescein, makes them as a suitable alternative when labeled biomolecules with a well-defined structure are required for biological applications. Work is in progress in our laboratory to increase the red-shifted properties of COUPY dyes with the aim of using them in ligand-targeted imaging applications such as fluorescence-guided surgery.

EXPERIMENTAL SECTION

Materials and Methods

Unless otherwise stated, common chemicals and solvents (HPLC grade or reagent grade quality) were purchased from commercial sources and used without further purification. Fmoc-protected amino acids, resins, and coupling reagents for solid-phase synthesis were obtained from Novabiochem, Bachem, or Iris Biotech. Fmoc-*L*-threoninol *p*-carboxyacetal was synthesized following previously reported procedures.[14] Solid-phase peptide synthesis (SPPS) was performed manually in a polypropylene syringe fitted with a polyethylene disk. Peptides were assembled on a Rink amide resin-*p*-MBHA (f = 0.50 mmol/g, 100−200 mesh) using standard Fmoc/^{t}Bu chemistry with the following side-chain protecting groups: Boc (N^{i}-*tert*-butoxicarbonyl, tryptophan, and N^{ε}-*tert*-butoxycarbonyl, lysine), ^{t}Bu (*O*-*tert*-butyl, threonine), and Trt (*S*-trityl, cysteine).

Aluminium plates coated with a 0.2 mm thick layer of silica gel 60 F_{254} were used for thin-layer chromatography analyses (TLC), whereas flash column chromatography purification was carried out using silica gel 60 (230-400 mesh). Reversed-phase high-performance liquid chromatography (HPLC) analyses were carried out on a Jupiter Proteo C_{18} column (250x4.6 mm, 90 Å 4 μm, flow rate: 1 mL/min) using linear gradients of 0.1% formic acid in H_2O (A) and 0.1% formic acid in ACN (B). NMR spectra were recorded at 25 ^{o}C in a 400 MHz spectrometer using the deuterated solvent as an internal deuterium lock. Tetramethylsilane (TMS) was used as an internal reference (0 ppm) for ^{1}H spectra recorded in $CDCl_3$ and the residual protic signal of the solvent (77.16 ppm) for ^{13}C spectra. The residual protic signal of DMSO was used as a reference in ^{1}H and ^{13}C NMR spectra recorded in DMSO-d_6. Chemical shifts are reported in part per million (ppm) in the δ scale, coupling constants in Hz and multiplicity as follows: s (singlet), d (doublet), t (triplet), q (quartet), qt (quintuplet), m (multiplet), dd (doublet of doublets), dt (doublet of triplets), ddd (doublet of doublet of doublets), br (broad signal), etc. The proton signals of the *E* and *Z* rotamers were identified by simple inspection of the ^{1}H spectrum and the rotamer ratio was calculated by peak integration. 2D-NOESY spectra were acquired in DMSO-d_6 with a mixing time of 500 ms. Electrospray ionization mass spectra (ESI-MS) were recorded on an instrument equipped with single quadrupole detector coupled to an HPLC, high-resolution (HR) ESI-MS on a LC/MS-TOF instrument.

Synthesis of compounds 9 and 10.

N-(3-Azidopropyl)-2-bromoacetamide (**9**). The published method with some modifications was followed to synthesize compound **9**.[15] 3-Azido-1-propanamine (250 mg, 2.5 mmol) was dissolved in 10 mL of DCM and then 10 mL of saturated aqueous $NaHCO_3$ were added. The mixture was vigorously stirred at -10 ºC and bromoacetyl bromide (1.01 g, 5.0 mmol) was slowly added. The reaction mixture was slowly allowed to warm to room temperature. After stirring for 3 h, the reaction mixture was partially concentrated to remove the organic solvent and then poured into 100 mL of water. The aqueous phase was extracted with AcOEt (2 x 100 mL), and the combined organic phases were washed with saturated $NaHCO_3$ (100 mL), 5 % aqueous HCl solution (100 mL) and saturated NaCl (100 mL). The organic phase was dried over anhydrous Na_2SO_4, filtered and evaporated under reduced pressure. The crude product was purified by column chromatography (silica gel, 0-60 % AcOEt in hexane) to give 364 mg of a pink oil (yield: 66 %). TLC: R_f (hexane/DCM 1:1) 0.5. ^{1}H NMR (400 MHz, $CDCl_3$) δ (ppm): 6.85 (1H, br s), 3.85 (2H, s), 3.37 (4H, m), 1.80 (2H, qt, J = 6.6 Hz). $^{13}C\{^1H\}$ NMR (101 MHz, $CDCl_3$) δ (ppm): 165.9, 49.3, 37.9, 29.1, 28.5. HRMS (ESI-TOF) *m/z*: $[M + H]^+$ Calcd for $C_5H_{10}BrN_4O$ 221.0033; Found 221.0027. MS (EI) *m/z* 220 (M^+, 5), 178 (10), 141 (25), 86 (70), 72 (100) (calcd mass for $C_5H_9{}^{79}BrN_4O$ $[M]^+$, 220; calcd mass for $C_5H_9{}^{81}BrN_4O$ $[M]^+$, 222).

*2-Bromo-N-(prop-2-yn-1-yl)acetamide (**10**).* The published method with some modifications was followed to synthesize compound **10**.[16] Propargylamine (500 mg, 9.1 mmol) was dissolved in 20 mL of DCM and then 20 mL of saturated aqueous $NaHCO_3$ were added. The mixture was vigorously stirred at -10 ºC and bromoacetyl bromide (3.66 g, 18.2 mmol) was slowly added. The reaction mixture was slowly allowed to warm to room temperature. After stirring for 3 h, the reaction mixture was partially concentrated to remove the organic solvent and then poured into 100 mL of water. The aqueous phase was extracted with AcOEt (2 x 100 mL), and the combined organic phases were washed with saturated $NaHCO_3$ (100 mL), 5 % aqueous HCl solution (100 mL) and saturated NaCl (100 mL). The organic phase was dried over anhydrous Na_2SO_4, filtered and evaporated under reduced pressure. The crude product was purified by column chromatography (silica gel, 0-60 % AcOEt in hexane) to give 0.87 g of a white solid (yield: 55 %). TLC: R_f (hexane/DCM 1:1) 0.5. ^{1}H NMR (400 MHz, $CDCl_3$) δ (ppm): 6.60 (1H, br s), 3.85 (2H, s), 4.09 (2H, dd, J = 5.6 Hz, J = 2.4 Hz), 3.90 (2H, s), 2.28 (1H, t, J = 2.4 Hz). $^{13}C\{^1H\}$ NMR (101 MHz, $CDCl_3$) δ (ppm): 165.2, 78.6, 72.4, 30.1, 28.8. HRMS (ESI-TOF) *m/z*: $[M + H]^+$ Calcd for C_5H_7BrNO 175.9706; Found 175.9708. MS (EI)

m/z 175 (M^+, 5), 96 (100), 82 (40), 39 (35) (calcd mass for $C_5H_6{}^{79}BrNO$ $[M]^+$, 175; calcd mass for $C_5H_6{}^{81}BrNO$ $[M]^+$, 177).

Synthesis of coumarin derivatives (4-6 and 8).

*2-(Cyano(1-(2-methoxy-(2-oxoethyl))(4-pyridin-1-ium))methylene)-7-(N,N-diethylamino)-4-methyl-coumarin bromide (**8**).* Methyl bromoacetate (140 µL, 1.51 mmol) was added to a solution of coumarin **2**[6a] (500 mg, 1.51 mmol) in AcOEt (60 mL). The mixture was stirred for 4 h at 60 ºC under an Ar atmosphere and protected from light. Then, methyl bromoacetate (140 µL, 1.51 mmol) was added again and the reaction mixture was stirred overnight at 60 ºC and protected from light. The crude product was evaporated under reduced pressure and purified by column chromatography (silica gel, 0-8% MeOH in DCM) to give 713 mg of purple solid (yield: 97 %). TLC: R_f (10% MeOH in DCM) 0.55. ^{1}H NMR (400 MHz, DMSO-d_6) δ (ppm): 8.59 (2H, d, *J* = 7.2 Hz), 8.17 (2H, d, *J* = 7.2 Hz), 7.70 (1H, d, *J* = 9.0 Hz), 7.04 (1H, d, *J* = 2.0 Hz), 6.96 (1H, dd, *J* = 9.0 Hz, *J* = 2.8 Hz), 6.89 (1H, s), 5.51 (2H, s), 3.78 (3H, s), 3.56 (4H, q, *J* = 7.2 Hz), 2.53 (3H, s), 1.18 (6H, t, *J* = 7.2 Hz). ^{13}C{^{1}H} NMR (101 MHz, DMSO-d_6) δ (ppm): 167.6, 166.8, 154.9, 153.2, 152.1, 149.6, 144.0, 127.0, 120.1, 118.0, 112.1, 110.4, 96.5, 78.2, 58.3, 53.0, 44.2, 18.5, 12.4. HRMS (ESI-TOF) *m/z*: $[M]^+$ Calcd for $C_{24}H_{26}N_3O_3$ 404.1969; Found 404.1963. Analytical HPLC (30 to 100% B in 30 min, formic acid additive): R_t = 7.3 min

*2-(Cyano(1-(carboxymethyl)(4-pyridin-1-ium))methylene)-7-(N,N-diethylamino)-4-methyl-coumarin chloride (**4**).* A 1:1 (v/v) mixture of HCl (37 %) and Milli-Q water (170 mL) was added to coumarin **8** (500 mg, 1.03 mmol). The reaction mixture was stirred for 5 h at 60 ºC under an Ar atmosphere and protected from light. After removal of the major part of the solvent, several co-evaporations from acetonitrile were carried out. The crude product was used without further purification since HPLC-MS analysis revealed that the hydrolysis reaction was quantitative. ^{1}H NMR (400 MHz, DMSO-d_6) δ (ppm): 8.59 (2H, d, *J* = 7.4 Hz), 8.18 (2H, d, *J* = 7.4 Hz), 7.72 (1H, d, *J* = 9.2 Hz), 7.04 (1H, br s), 6.98 (1H, dd, *J* = 9.2 Hz, *J* = 2.4 Hz), 6.93 (1H, d, *J*=2.4 Hz), 5.39 (2H, s), 3.56 (4H, q, *J* = 7.2 Hz), 2.55 (3H, s), 1.18 (6H, t, *J* = 7.2 Hz). HRMS (ESI-TOF) *m/z*: $[M]^+$ Calcd for $C_{23}H_{24}N_3O_3$ 390.1812; Found 390.1808. Analytical HPLC (30 to 100% B in 30 min, formic acid additive): R_t = 10.2 min).

*2-(Cyano(1-(2-((3-azidopropyl)amino)-2-oxoethyl))(4-pyridin-1-ium))methylene)-7-(N,N-diethylamino)-4-methyl-coumarin bromide (**5**).* *N*-(3-Azidopropyl)-2-bromoacetamide (167 mg, 0.75 mmol) was added to a solution of coumarin **2**[6a] (250 mg, 0.75 mmol) in a 1:1 mixture of AcOEt and ACN (30 mL), which was previously heated at 50 ºC. After stirring for 2 h at 50 ºC, an additional amount of compound **9** (167 mg, 0.75 mmol) was added and the

reaction mixture was stirred for 5 h at 50 ºC. After evaporation under reduced pressure and purification by column chromatography (silica gel, 0-6% MeOH in DCM), 400 mg of a dark purple solid were obtained (yield: 96 %). TLC: R_f (10% MeOH in DCM) 0.45. ^{1}H NMR (400 MHz, DMSO-d_6) δ (ppm): 8.58 (1H, t, *J* = 5.6 Hz), 8.53 (2H, d, *J* = 7.4 Hz), 8.16 (2H, d, *J* = 7.4 Hz), 7.72 (1H, d, *J* = 9.2 Hz), 7.01 (1H, br s), 6.98 (1H, dd, *J* = 9.2 Hz, *J* = 2.4 Hz), 6.93 (1H, s), 5.24 (2H, s), 3.56 (4H, q, *J* = 7.2 Hz), 3.41 (2H, t, *J* = 6.8 Hz), 3.21 (2H, q, *J* = 6.8 Hz), 2.55 (3H, s), 1.71 (2H, qt, *J* = 6.8 Hz), 1.18 (6H, t, *J* = 7.2 Hz). ^{13}C{^{1}H} NMR (101 MHz, DMSO-d_6) δ (ppm): 166.8, 165.0, 154.9, 152.8, 152.0, 149.2, 144.2, 127.0, 120.0, 118.2, 111.9, 110.4, 96.4, 78.1, 59.5, 54.9, 48.2, 44.2, 36.3, 28.2, 18.4, 12.3. HRMS (ESI-TOF) *m/z*: $[M]^+$ Calcd for $C_{26}H_{30}N_7O_2$ 472.2455; Found 472.2450. Analytical HPLC (30 to 100% B in 30 min, formic acid additive): R_t = 8.0 min.

*2-(Cyano(1-(2-oxo-2-(prop-2-yn-1-ylamino)ethyl))(4-pyridin-1-ium))methylene)-7-(N,N-diethylamino)-4-methyl-coumarin bromide (**6**).* 2-Bromo-*N*-(prop-2-yn-1-yl)acetamide (**10**) (42 mg, 0.75 mmol) was added to a solution of coumarin **2**[6a] (250 mg, 0.75 mmol) in a 1:1 mixture of AcOEt and ACN (30 mL), which was previously heated at 50 ºC. After stirring for 2 h at 50 ºC, an additional amount of compound **9** (63 mg, 1.12 mmol) was added and the reaction mixture was stirred overnight at 50 ºC. After evaporation under reduced pressure and purification by column chromatography (silica gel, 0-6% MeOH in DCM), 304 mg of a dark purple solid were obtained (yield: 80 %). TLC: R_f (10% MeOH in DCM) 0.60. ^{1}H NMR (400 MHz, DMSO-d_6) δ (ppm): 9.01 (1H, t, *J* = 5.6 Hz), 8.53 (2H, d, *J* = 7.4 Hz), 8.16 (2H, d, *J* = 7.4 Hz), 7.72 (1H, d, *J* = 9.2 Hz), 7.01 (1H, br s), 6.98 (1H, dd, *J* = 9.2 Hz, *J* = 2.4 Hz), 6.93 (1H, s), 5.27 (2H, s), 3.98 (2H, dd, *J* = 5.6 Hz, *J* = 2.4 Hz), 3.57 (4H, q, *J* = 7.2 Hz), 3.23 (1H, t, *J* = 2.4 Hz), 2.55 (3H, s), 1.18 (6H, t, *J* = 7.2 Hz). ^{13}C{^{1}H} NMR (101 MHz, DMSO-d_6) δ (ppm): 166.8, 165.0, 154.9, 152.9, 152.0, 149.3, 144.2, 127.0, 120.0, 118.2, 111.9, 110.5, 110.4, 96.4, 80.3, 78.1, 73.8, 59.3, 44.2, 28.4, 18.4, 12.4. HRMS (ESI-TOF) *m/z*: $[M]^+$ Calcd for $C_{26}H_{27}N_4O_2$ 427.2129; Found 427.2127. Analytical HPLC (30 to 100% B in 30 min, formic acid additive): R_t = 7.3 min.

Synthesis and characterization of COUPY-octreotide conjugate 12

*Fmoc-NH-PEG-D-Phe-Cys(Trt)-Phe-D-Trp(Boc)-Lys(Boc)-Thr(tBu)-Cys(Trt)-Thr(ol)-Resin (**11**).* Octreotide-bound resin **11** was prepared following previously reported procedures.[9b] Briefly, the Fmoc-protected *L*-threoninol functionalized as the *p*-carboxybenzaldehyde acetal was anchored to the solid support by using DIPC (3 mol equiv) and HOBt (3 mol equiv) in anhydrous DMF for 3 h and, subsequently, the following Fmoc-protected amino acids as well as the Fmoc-protected PEG spacer, 8-(9-fluorenylmethyloxycarbonyl-amino)-3,6-

dioxaoctanoic acid, were incorporated using DIPC (3 mol equiv) and HOAt (3 mol equiv) in anhydrous DMF for 2 h.

*COUPY-octreotide conjugate (**12**).* After removal of the Fmoc protecting group from peptide-bound resin **11** with 20 % piperidine in DMF (2 x 10 min), coumarin **4** (4 mol equiv.) was coupled by using HATU (3.9 mol equiv.) and DIPEA (2+2 mol equiv.) in anhydrous DMF for 3 h in the dark by using the following procedure: DIPEA (2 mol equiv.) was first added to a solution of coumarin **4** and HATU in anhydrous DMF and, after stirring for 5 min a RT, the mixture was added to DMF-swollen peptide-bound resin **11**; then, DIPEA (2 mol equiv.) was immediately added and the reaction mixture was stirred for 2 h. Cleavage and deprotection of the resulting COUPY-octreotide-bound resin were simultaneously performed by treatment with TFA/H_2O/EDT/TIS 94:2.5:2.5:1 for 2.5 h at RT and protected from light. Most of the TFA was removed by bubbling N_2 into the solution, and the resulting residue was poured onto cold diethyl ether to precipitate the target compound. The solid was isolated by centrifugation, dissolved in H_2O/ACN (9:1) and lyophilized. Cyclisation was accomplished after continuously stirring an aerated solution of the crude material in a 97:3 (v/v) mixture of aqueous NH_4HCO_3 (5%) pH 7-8 and DMSO overnight at RT (1 mL solution per 1 mg of theoretical peptide). As shown in Figure S5, analytical reversed-phase HPLC-MS analysis (10 to 70% B in 30 min, 0.1 % formic acid additive) revealed the presence of a main peak that was characterized as the expected COUPY-octreotide conjugate **12** (R_t = 15.6 min). The solution was lyophilized and the conjugate purified by semipreparative RP-HPLC (gradient from 45 to 70% B in 30 min, A: 0.045 % TFA in H_2O, B: 0.1% TFA in ACN, flow rate: 3 mL/min, R_t = 6 min). Overall yield (synthesis + purification): 2.35 mg of a purple solid (from 27 mg of resin **11**), 12%. HRMS (ESI-TOF) *m/z*: $[M]^+$ Calcd for $C_{78}H_{99}N_{14}O_{15}S_2$ 1535.6850; Found 1535.6844; *m/z*: $[M + H]^{2+}$ Calcd for $C_{78}H_{100}N_{14}O_{15}S_2$ 768.3462; Found 768.3469. Analytical RP-HPLC (10 to 70% B in 30 min; A, 0.1% formic acid in H_2O; B, 0.1% formic acid in ACN; R_t = 15.6 min).

Synthesis and characterization of COUPY-octreotide conjugates 15 and 16

*Alkynyl-PEG-D-Phe-Cys(Trt)-Phe-D-Trp(Boc)-Lys(Boc)-Thr(tBu)-Cys(Trt)-Thr(ol)-Resin (**13**).* After removal of the Fmoc protecting group from the peptide-bound resin **11** with 20 % piperidine in DMF (2 x 10 min), 4-pentynoic acid (5 mol equiv.) was coupled by using DIPC (5 mol equiv.) and HOAt (5 mol equiv.) in anhydrous DMF for 2 h. Cleavage and deprotection of an aliquot of the resulting octreotide-bound resin **13** was performed by treatment with TFA/H_2O/EDT/TIS 94:2.5:2.5:1 for 2.5 h. After evaporation of TFA by bubbling with N_2, the crude peptide was precipitated with cold diethyl ether. As shown in

Figure S9, reversed-phase HPLC-MS analysis showed the presence of two peaks that were characterized as the linear alkynyl-octreotide (R_t = 15.2 min) and the corresponding disulfide cyclized alkynyl-octreotide (R_t = 14.8 min). Linear alkynyl-octreotide: LR-ESI MS, positive mode: *m/z* 1246.54 (calcd mass for $C_{60}H_{84}N_{11}O_{14}S_2$ $[M+H]^+$: 1246.56). Analytical HPLC (10 to 70% B in 30 min, 0.1 % formic acid additive): R_t = 15.2 min. Disulfide cyclized alkynyl-octreotide: LR-ESI MS, positive mode: *m/z* 1244.71 (calcd mass for $C_{60}H_{82}N_{11}O_{14}S_2$ $[M+H]^+$: 1244.55). Analytical HPLC (10 to 70% B in 30 min, 0.1 % formic acid additive): R_t = 14.7 min.

*Azido-PEG-D-Phe-Cys(Trt)-Phe-D-Trp(Boc)-Lys(Boc)-Thr(tBu)-Cys(Trt)-Thr(ol)-Resin (**14**).* After removal of the Fmoc protecting group from the peptide-bound resin **11** with 20 % piperidine in DMF (2 x 10 min), 2-azidoacetic acid (5 mol equiv.) was coupled by using DIPC (5 mol equiv.) and HOAt (5 mol equiv.) in anhydrous DMF for 2 h. Cleavage and deprotection of an aliquot of the resulting octreotide-bound resin **14** was performed by treatment with TFA/H_2O/EDT/TIS 94:2.5:2.5:1 for 2.5 h. After evaporation of TFA by bubbling with N_2, the crude peptide was precipitated with cold diethyl ether. As shown in Figure S10, reversed-phase HPLC-MS analysis showed the presence of two peaks that were characterized as the linear azido-octreotide (R_t = 15.2 min) and the corresponding disulfide cyclized azido-octreotide (R_t = 14.7 min). Linear azido-octreotide: LR-ESI MS, positive mode: *m/z* 1249.50 (calcd mass for $C_{57}H_{81}N_{14}O_4S_2$ $[M+H]^+$: 1249.55). Analytical HPLC (10 to 70% B in 30 min, 0.1 % formic acid additive): R_t = 15.2 min. Disulfide cyclized azido-octreotide: LR-ESI MS, positive mode: *m/z* 1247.48 (calcd mass for $C_{57}H_{79}N_{14}O_4S_2$ $[M+H]^+$: 1247.53). Analytical HPLC (10 to 70% B in 30 min, 0.1 % formic acid additive): R_t = 14.7 min.

*COUPY-octreotide conjugate (**15**).* 5 mg of alkynyl-peptide-bound resin **13** were transferred to a 2 mL reaction vial equipped with a magnetic stirrer. Afterwards, a solution of azido-coumarin **5** (4.2 mg, 3 mol equiv.), $CuSO_4$ (1.2 mg, 3 mol equiv.) and sodium ascorbate (1.5 mg, 3 mol equiv.) in 800 µL DMF/$H_2$0 20:1 (v/v) was immediately added to the vial. The suspension was allowed to stir at room temperature for 1 h, 4 h or overnight under argon atmosphere in the dark. Then, the resin was filtered off and washed with DMF, DCM and MeOH (5,5,5 x 4 mL). Cleavage, deprotection and cyclisation were carried out as described above for conjugate **12**. As shown in Figure S9, analytical reversed-phase HPLC-MS analysis (10 to 70% B in 30 min, 0.1 % formic acid additive) revealed the presence of a main peak in the three cases that was characterized as the expected COUPY-octreotide conjugate **15** (R_t = 15.4 min). The solution was lyophilized and the conjugate purified by semipreparative RP-

HPLC (gradient from 45 to 100% B in 30 min, A: 0.1 % TFA in H_2O, B: 0.1% TFA in ACN, flow rate: 3 mL/min, R_t = 6.5 min). Overall yield (synthesis + purification): 5.23 mg of a purple solid (from 15 mg of resin **13**), 32%. HRMS (ESI-TOF) *m/z*: $[M]^+$ Calcd for $C_{86}H_{111}N_{18}O_{16}S_2$ 1715.7861; Found 1715.7912; *m/z*: $[M + H]^{2+}$ Calcd for $C_{86}H_{112}N_{18}O_{16}S_2$ 858.3970; Found 858.3973. Analytical RP-HPLC (10 to 70% B in 30 min; A, 0.1% formic acid in H_2O; B, 0.1% formic acid in CAN): R_t = 15.4 min.

*COUPY-octreotide conjugate (**16**).* 5 mg of azido-peptide-bound resin **14** were transferred to a 2 mL reaction vial equipped with a magnetic stirrer. Afterwards, a solution of alkynyl-coumarin **6** (3.8 mg, 3 mol equiv.), $CuSO_4$.(1.2 mg, 3 mol equiv.) and sodium ascorbate (1.5 mg, 3 mol equiv.) in 800 µL DMF/$H_2$0 20:1 (v/v) was immediately added to the vial. The suspension was allowed to stir at room temperature for 1 h, 4 h or overnight under argon atmosphere in the dark. Then, the resin was filtered off and washed with DMF, DCM and MeOH (5,5,5 x 4 mL). Cleavage, deprotection and cyclisation were carried out as described above for conjugate **12**. As shown in Figure S11, analytical reversed-phase HPLC-MS analysis (10 to 70% B in 30 min, 0.1 % formic acid additive) revealed the presence of a main peak in the three cases that was characterized as the expected COUPY-octreotide conjugate **16** (R_t = 15.3 min). The solution was lyophilized and the conjugate purified by semipreparative RP-HPLC (gradient from 45 to 100% B in 30 min, A: 0.1 % TFA in H_2O, B: 0.1% TFA in ACN, flow rate: 3 mL/min, R_t = 6.5 min). Overall yield (synthesis + purification): 5.23 mg of a purple solid (from 20 mg of resin **14**), 13%. HRMS (ESI-TOF) *m/z*: $[M]^+$ Calcd for $C_{83}H_{105}N_{18}O_{16}S_2$ 1673.7392; Found 1673.7388; *m/z*: $[M + H]^{2+}$ Calcd for $C_{83}H_{106}N_{18}O_{16}S_2$ 837.3750; Found 837.3735. Analytical RP-HPLC (10 to 70% B in 30 min; A, 0.1% formic acid in H_2O; B, 0.1% formic acid in ACN): R_t = 15.3 min.

Synthesis and characterization of Atto-Rho12-octreotide conjugate (17).

Octreotide acetate (Bachem; 1 mg, 0.98 µmol) was allowed to react with Atto Rho12-hexanoic acid *N*-hydroxysuccinimide ester (ATTO Tech; 1 mg, 1.18 µmol) in an aqueous hydrogencarbonate buffer (100 mM, pH 7.5) for 3 h and protected from light. The solution was lyophilized and Atto-Rho12-octreotide conjugate (**17**) was purified by analytical RP-HPLC (gradient from 30 to 100 % in 30 min; A: 0.1 % formic acid in H_2O, B: 0.1% formic acid in ACN, flow rate: 1 mL/min, R_t = 16.7 min). Overall yield (synthesis + purification): 0.4 mg of a pink solid, 25%. Characterization: LR ESI MS, positive mode: *m/z* 1651.65 (calcd mass for $C_{90}H_{116}N_{13}O_{13}S_2^+$: 1650.82).

Photophysical characterization of the compounds.

Absorption spectra were recorded in a Varian Cary 500 UV/Vis/NIR spectrophotometer at room temperature. Molar absorption coefficients (ε) were determined by direct application of the Beer-Lambert law, using solutions of the compounds in each solvent with concentrations ranging from 10^{-6} to 10^{-5} M. Emission spectra were registered in a Photon Technology International (PTI) fluorimeter. Fluorescence quantum yields (Φ_F) were measured by comparative method using cresyl violet in ethanol (CV; $\Phi_{F;Ref} = 0.54 \pm 0.03$) as reference.[17] Then, optically-matched solutions of the compounds and CV were excited and the fluorescence spectra was recorded. The absorbance of sample and reference solutions was set below 0.1 at the excitation wavelength and Φ_F were calculated using the following equation (1):

$$\phi_{F;Sample} = \frac{Area_{Sample}}{Area_{Ref}} x \left(\frac{\eta_{Sample}}{\eta_{Ref}}\right)^2 x\, \phi_{F;ref} \quad (1)$$

where $Area_{Sample}$ and $Area_{Ref}$ are the integrated fluorescence for the sample and the reference and η_{Sample} and η_{Ref} are the refractive index of sample and reference solutions respectively. The uncertainty in the experimental value of Φ_F has been estimated to be approximately 10%.

Photostability studies were performed by monitoring fluorescence bleaching of a 5 μM aqueous solution (PBS buffer) of the compounds irradiated with a high power LED of 505 nm (100 mW/cm^2).

Cell culture and treatments

HeLa Cells were maintained in DMEM (Dullbecco Modified Eagle Medium) containing low glucose (1 g/L) and supplemented with 10% foetal calf serum (FCS), 50U/mL penicillin-streptomycin and 2 mM *L*-glutamine. For cellular uptake experiments and posterior observation under the microscope, cells were seeded on glass bottom dishes (P35G-1.5-14-C, Mattek). 24 h after cell seeding, cells were incubated for 30 min or 1 h at 37 ºC with coumarin **3** (0.5 μM), COUPY-octreotide **12** (10 μM), Atto Rho12-octreotide **17** (10 μM) or Fluorescein-octreotide **18** (50 μM) in supplemented DMEM. Then, cells were washed three times with DPBS (Dulbecco's Phosphate-Buffered Saline) to remove the excess of the compounds and kept in low glucose DMEM without phenol red for fluorescence imaging.

Fluorescence imaging

All microscopy observations were performed using a Zeiss LSM 880 confocal microscope equipped with a 405 nm laser diode, an Argon-ion laser, a 561 nm laser and a 633 nm laser. The microscope was also equipped with a full enclosure imaging chamber (XLmulti S1,

Pecon) connected to a 37 ºC heater and a 5% CO_2 providing system. Cells were observed using a 63X 1.2 multi immersion objective. Compounds **3**, **12** and **17** were excited using the 561 nm laser and detected from 570 to 670 nm. Compound **18** was observed using the 488 nm laser line of the Argon-ion laser. Image analysis was performed using Fiji.[18] Unless otherwise stated images are colorized using Fire lookup table.

ASSOCIATED CONTENT

Supporting Information

Copies of HPLC traces and UV−vis absorption and fluorescence emission spectra of the compounds; additional fluorescence imaging studies; 1D NMR (^{1}H, ^{13}C, and ^{19}F), MS, and selected 2D NMR spectra.

This material is available free of charge via the Internet at http://pubs.acs.org.

AUTHOR INFORMATION

Corresponding Author

*E-mail: vmarchan@ub.edu

ACKNOWLEDGEMENTS

This work was supported by funds from the Spanish *Ministerio de Economía y Competitividad* (grants CTQ2014-52658-R and CTQ2017-84779-R). The authors acknowledge helpful assistance of Dr. Francisco Cárdenas (NMR) and Dr. Irene Fernández and Laura Ortiz (MS) from CCiTUB. A.G. was a recipient fellow of the University of Barcelona.

REFERENCES

(1) (a) Srinivasarao, M.; Galliford, C. V.; Low, P. S. Principles in the design of ligand-targeted cancer therapeutics and imaging agents. *Nat. Rev. Drug Discovery.* **2015**, *14*, 203-219; (b) Zhang, R. R.; Schroeder, A. B.; Grudzinski, J. J.; Rosenthal, E. L.; Warram, J. M.; Pinchuk, A. N.; Eliceiri, K. W.; Kuo, J. S.; Weichert, J. P. Beyond the margins: real-time detection of cancer using targeted fluorophores. *Nat. Rev. Clin. Oncol.* **2017**, *14*, 347-364.

(2) (a) Owens, E. A.; Henary, M.; El Fakhri, G.; Soo Choi, H. Tissue-Specific Near-Infrared Fluorescence Imaging. *Acc. Chem. Res.* **2016**, *49*, 1731-1740; (b) Guo, Z.; Park, S.; Yoon, J.; Shin, I. Recent progress in the development of near-infrared fluorescent probes for bioimaging applications. *Chem. Soc. Rev*. **2014**, *43*, 16-29; c) Haque, A.; Faizi, M. S. H.;

Rather, J. A.; Khan, M. S. Next generation NIR fluorophores for tumor imaging and fluorescence-guided surgery: A review. *Bioorg. Med. Chem.* 2017, **25**, 2017-2034.

(3) Gao, M.; Yu, F.; Lv, C.; Choo, J.; Chen, L. Fluorescent chemical probes for accurate tumor diagnosis and targeting therapy. *Chem. Soc. Rev*. **2017**, *46*, 2237-2271.

(4) (a) Birch, D.; Christensen, M. V.; Staerk, D.; Franzyk, H.; Nielsen, H. M. Fluorophore labeling of a cell-penetrating peptide induces differential effects on its cellular distribution and affects cell viability. *BBA Biomembranes* **2017**, *1859*, 2483-2494; (b) Zhao, C.; Fernandez, A.; Avlonitis, N.; Vande Velde, G.; Bradley, M.; Read, N. D.; Vendrell, M. Searching for the Optimal Fluorophore to Label Antimicrobial Peptides. *ACS Comb. Sci*. **2016**, *18*, 689-696.

(5) (a) Sato, K.; Gorka, A. P.; Nagaya, T.; Michie, M. S.; Nakamura, Y.; Nani, R. R.; Coble, V. L.; Vasalatiy, O. V.; Swenson, R. E.; Choyke, P. L.; Schnermann, M. J.; Kobayashi, H. Effect of charge localization on the in vivo optical imaging properties of near-infrared cyanine dye/monoclonal antibody conjugates. *Mol. BioSyst*. **2016**, *12*, 3046-3056; (b) Zhao, N.; Williams, T. M.; Zhou, Z.; Fronczek, F. R.; Sibrian-Vazquez, M.; Jois, S. D.; Vicente, M. G. H. Synthesis of BODIPY-Peptide Conjugates for Fluorescence Labeling of EGFR Overexpressing Cells. *Bioconjugate Chem*. **2017**, *28*, 1566-1579.

(6) (a) Gandioso, A.; Bresolí-Obach, R.; Nin-Hill, A.; Bosch, M.; Palau, M.; Galindo, A.; Contreras, S.; Rovira, A.; Rovira, C.; Nonell, S.; Marchán, V. Redesigning the Coumarin Scaffold into Small Bright Fluorophores with Far-Red to Near-Infrared Emission and Large Stokes Shifts Useful for Cell Imaging. *J. Org. Chem*. **2018**, *83*, 1185-1195; (b) Gandioso, A.; Palau, M.; Bresolí-Obach, R.; Galindo, A.; Rovira, A.; Bosch, M.; Nonell, S.; Marchán, V. High Photostability in Nonconventional Coumarins with Far-Red/NIR Emission through Azetidinyl Substitution. *J. Org. Chem*. **2018**, *83*, 11519-11531.

(7) (a) Shank, N. I.; Pham, H. H.; Waggoner, A. S.; Armitage, B. A. Twisted Cyanines: A Non-Planar Fluorogenic Dye with Superior Photostability and its Use in a Protein-Based Fluoromodule. *J. Am. Chem. Soc*. **2013**, *135*, 242-251; (b) Bohlaender, P. R.; Wagenknecht, H.-A. Synthesis of a Photostable Energy-Transfer Pair for "DNA Traffic Lights". *Eur. J. Org. Chem.* **2014**, *34*, 7547-7551.

(8) Pickens, C. J.; Johnson, S. N.; Pressnall, M. M.; Leon, M. A.; Berkland, C. J. Practical Considerations, Challenges, and Limitations of Bioconjugation via Azide-Alkyne Cycloaddition. *Bioconjugate Chem*. **2018**, *29*, 686-701.

(9) (a) Mezo, G.; Manea, M. Receptor-mediated tumor targeting based on peptide hormones. *Expert Opin. Drug Delivery* **2010**, *7*, 79-96; (b) Janecka, A.; Zubrzycka, M.; Janecki, T.

Somatostatin analogs. *J. Pept. Res*. **2001**, *58*, 91-107; (c) Reubi, J. C. Peptide receptors as molecular targets for cancer diagnosis and therapy. *Endocr. Rev*. **2003**, *24*, 389-427.

(10) (a) Sun, L.-C.; Coy, D. H. Cytotoxic conjugates of peptide hormones for cancer chemotherapy. *Drugs Future* **2008**, *33*, 217-223; (b) Barragán, F.; Carrion-Salip, D.; Gómez-Pinto, I.; González-Cantó, C.; Sadler, P. J.; de Llorens, R.; Moreno, V.; González, C.; Massaguer, A.; Marchán, V. Somatostatin Subtype-2 Receptor-Targeted Metal-Based Anticancer Complexes. *Bioconjugate Chem*. **2012**, *23*, 1838-1855; (c) Barragan, F.; Moreno, V.; Marchán, V. Solid-phase synthesis and DNA binding studies of dichloroplatinum(ii) conjugates of dicarba analogues of octreotide as new anticancer drugs. *Chem. Commun*. **2009**, 4705-4707.

(11) Novohradsky, V.; Zamora, A.; Gandioso, A.; Brabec, V.; Ruiz, J.; Marchán, V. Somatostatin receptor-targeted organometallic iridium(iii) complexes as novel theranostic agents. *Chem. Commun*. **2017**, *53*, 5523-5526.

(12) (a) Gandioso, A.; Palau, M.; Nin-Hill, A.; Melnyk, I.; Rovira, C.; Nonell, S.; Velasco, D.; García-Amorós, J.; Marchán, V. Sequential Uncaging with Green Light can be Achieved by Fine-Tuning the Structure of a Dicyanocoumarin Chromophore. *ChemistryOpen* **2017**, *6*, 375-384; (b) Gandioso, A.; Contreras, S.; Melnyk, I.; Oliva, J.; Nonell, S.; Velasco, D.; García-Amorós, J.; Marchán, V. Development of Green/Red-Absorbing Chromophores Based on a Coumarin Scaffold That Are Useful as Caging Groups. *J. Org. Chem*. **2017**, *82*, 5398-5408.

(13) (a) Castro, V.; Rodríguez, H.; Albericio, F. CuAAC: An Efficient Click Chemistry Reaction on Solid Phase. *ACS Comb. Sci*. **2016**, *18*, 1-14; (b) Song, X.; Wang, C.; Han, Z.; Xu, Y.; Xiao, Y. Terminal alkyne substituted O6-benzylguanine for versatile and effective syntheses of fluorescent labels to genetically encoded SNAP-tags. *RSC Adv*. **2015**, *5*, 23646-23649; (c) Yang, F.; Wang, C.; Wang, L.; Ye, Z.-W.; Song, X.-B.; Xiao, Y. Hoechst-naphthalimide dyad with dual emissions as specific and ratiometric sensor for nucleus DNA damage. *Chin. Chem. Lett*. **2017**, *28*, 2019-2022; (d) Wang, C.; Song, X.; Han, Z.; Li, X.; Xu, Y.; Xiao, Y. Monitoring Nitric Oxide in Subcellular Compartments by Hybrid Probe Based on Rhodamine Spirolactam and SNAP-tag. ACS Chem. Biol. **2016**, *11*, 2033-2040.

(14) H.-P. Hsieh, Y.-T. Wu, S.-T. Chen, K.-T. Wang. Direct solid-phase synthesis of octreotide conjugates: precursors for use as tumor-targeted radiopharmaceuticals. *Bioorg. Med. Chem*. **1999**, *7*, 1797-1803.

(15) Sneddon, D.; Niemans, R.; Bauwens, M.; Yaromina, A.; van Kuijk, S. J. A.; Lieuwes, N. G.; Biemans, R.; Pooters, I.; Pellegrini, P. A.; Lengkeek, N. A.; Greguric, I.; Tonissen, K. F.;

Supuran, C. T.; Lambin, P.; Dubois, L.; Poulsen, S.-A. Synthesis and in vivo biological evaluation of 68Ga-labeled carbonic anhydrase IX targeting small molecules for positron emission tomography. *J. Med. Chem.* **2016**, *59*, 6431-6443.

(16) Goswami, L. N.; Cai, Q.; Ma, L.; Jalisatgi, S. S.; Hawthorne, M. F. Synthesis, relaxation properties and in vivo assessment of a carborane-GdDOTA-monoamide conjugate as an MRI blood pool contrast agent. *Org. Biomol. Chem.* **2015**, *13*, 8912-8918.

(17) Magde, D.; Brannon, J. H.; Cremers, T. L.; Olmsted, J. Absolute luminescence yield of cresyl violet. A standard for the red. *J. Phys. Chem.* **1979**, *83*, 696-699.

(18) Schindelin, J.; Arganda-Carreras, I.; Frise, E.; Kaynig, V.; Longair, M.; Pietzsch, T.; Preibisch, S.; Rueden, C.; Saalfeld, S.; Schmid, B.; Tinevez, J. Y.; White, D. J.; Hartenstein, V.; Eliceiri, K.; Tomancak, P.; Cardona, A. Fiji: an open-source platform for biological-image analysis. *Nat. Methods* **2012**, *9*, 676-682.